(22) Shibayama, M.; Hashimoto, T. *Macromolecules* **1986**, *19*, 740.
(23) Hasegawa, H.; Hashimoto, T. *Macromolecules* **1985**, *18*, 589.
(24) Inoue, T.; Moritani, M.; Hashimoto, T.; Kawai, H. *Macromolecules* **1971**, *4*, 500.
(25) It is said that there is about 0.3% error in the elementary analysis measurement. This implies that the composition obtained from the elementary analysis involves 7.3% error since the difference in the weight fractions of carbon (or hydrogen) atoms between styrene and isoprene monomeric units is 4.1%. Nevertheless, we believe that the error in the composition is within 1% or 2% when PI content is not so high because the elementary analysis results are reproducible within less than 0.1% of error and also because we usually observe an excellent agreement between the composition thus obtained and that obtained from the analyses of SAXS profiles of lamellar type.[22,26]
(26) Hasegawa, H.; Hashimoto, T. *Kobunshi Ronbunshu*, **1984**, *41*, 759.
(27) This statement may be confusing because in the bulk state solvent removal is more tedious for a material below its T_g than a material above its T_g and at room temperature PS is below its T_g and PI is above its T_g. However, the samples for elemental analysis are usually freeze-dried for faster and more effective removal of the solvent. In this case T_g gives the opposite effect; i.e., PS can maintain a porous structure, which makes solvent removal easier, while a porous structure in PI tends to collapse as the sample temperature increases in the drying process, making complete removal of the solvent very difficult.
(28) Inoue, T.; Soen, T.; Hashimoto, T.; Kawai, H. *J. Polym. Sci., Part A-2* **1969**, *7*, 1283.
(29) Kinning, D. J.; Thomas, E. L.; Alward, D. B.; Fetters, L. J.; Handlin, D. L., Jr. *Macromolecules* **1986**, *19*, 1288.
(30) Helfand, E.; Wasserman, Z. R. In *Developments in Block Copolymers*; Goodman, I., Ed.; Applied Science: Essex, U.K., 1984.
(31) Leibler, L. *Macromolecules* **1980**, *13*, 1602.
(32) Hashimoto, T.; Fujimura, M.; Kawai, H. *Macromolecules* **1980**, *13*, 1660.
(33) Mori, K.; Hasegawa, H.; Hashimoto, T., to be published.
(34) In other words, the occurrence of a morphological transition depends on whether the system is in the strong segregation limit or in the weak segregation limit. According to our unpublished results, the order-disorder transition takes place at ca. 200 °C for PS-PI diblock polymer with $M_n = 3.3 \times 10^4$ and the weight fraction of PS being 0.3. In this case annealing at higher temperatures close to 200 °C might change the morphology (from a nonequilibrium to an equilibrium one). The morphological transition below the order-disorder transition temperature may be possible in some cases if the molecular weights of the block polymers are small. But such a transition is not well understood and left for future investigations.
(35) The thickness of the ultrathin section was measured by the electron microscopy of the folded specimen, the technique proposed by: Adachi, K.; Adachi, M.; Kato, M.; Fukami, A. *Proc. Jpn. Electron Microsc. Soc., 21st* **1965**, 116.
(36) Tilting a specimen under the electron microscope cannot reveal the three-dimensional structure effectively when the thickness of the specimen is smaller than the lattice spacing, since the specimen does not contain the entire unit cell.
(37) This "wagon-wheel" image is different from those reported for the star block polymers simply because the contrast is reversed. However, because of its characteristic appearance we call it also a "wagon-wheel" image.
(38) Hashimoto, T. *Macromolecules* **1982**, *15*, 1548.
(39) Hasegawa, H.; Yamasaki, K.; Hashimoto, T., to be published.
(40) Hasegawa, H.; Hashimoto, T. *Macromolecules* **1985**, *18*, 589.
(41) The order-disorder transition temperature estimated for HY-10 is ca. 550 °C, which is far beyond the degradation temperature of this polymer. Therefore a morphological transition by annealing at a practical temperature cannot be expected for this polymer because the system is in the strong segregation limit and the kinetic barriers are too large.
(42) Burrel, H. *Polymer Handbook*, 2nd ed.; Brandrup, J., Immergut, E. H., Eds.; Wiley: New York, 1975.
(43) Lamellar, cylindrical, and spherical morphologies were successfully obtained from the block polymers having a tetrapod-network structure by changing the selectivity of the casting solvent. However, there has been no success so far in obtaining the tetrapod-network morphology from block polymers having spherical, cylindrical, or lamellar morphology as their equilibrium morphology either by changing the selectivity of the casting solvent or by solubilizing the homopolymer of one component which increases the volume fraction of the corresponding microphase. This may be a key to understanding the physics of the tetrapod morphology and is a subject for future work.
(44) The SAXS intensity distributions for the films cast from toluene, styrene, and 1,4-dioxane are circularly symmetrical with respect to the incident beam axis.
(45) Thomas, E. L.; Kinning, D. J., private communication.
(46) Hasegawa, H.; Hashimoto, T.; Kinning, D. J.; Thomas, E. L.; Fetters, L. J., to be published.
(47) Hasegawa, H., unpublished results.
(48) Unfortunately Figure 12 is reduced in size from the original figure prepared for the stereovision by a factor of 2.2. One should enlarge the picture by this factor for the real stereovision.

Molecular Structure and Elastic Behavior of Poly(ethylene oxide) Networks Swollen to Equilibrium

Yves Gnanou, Gérard Hild, and Paul Rempp*

Institut Charles Sadron (CRM-EAHP) (CNRS-ULP), 67083 Strasbourg Cedex, France.
Received October 6, 1986

ABSTRACT: Poly(ethylene oxide) (PEO) networks are prepared by an end-linking procedure upon reacting α,ω-dihydroxy PEO chains with a plurifunctional isocyanate in stoichiometric amounts. The networks obtained are characterized by their equilibrium swelling degree in dioxane and in water and by the elastic modulus arising from uniaxial compression measurements. For each network, utilizing the Miller-Macosko theory, we have calculated the effective structural parameters, ν, the number of elastically active chains, and μ, the number of junctions, and the trapping factor Te. This enabled us to compare the predictions originating from the various theories of rubber elasticity with our experimental data. It appears that both the limitation of junction fluctuations *and* the trapped entanglements are to be considered to account for the behavior of the swollen PEO networks in the range of small strains.

Introduction

The elastomeric behavior of networks has been investigated for a long time. Much effort has been devoted to relating their elastic response to their molecular structure. The various molecular theories of rubber elasticity rest on the premise that the stress in a deformed elastomer originates from the strain of the elastic chains. The elastic free energy stored (the calculation of which is a key problem) is the sum of contributions of the individual network chains. To test these theories, quantitative and independent information on the structure of the gels (such as molecular weight of the chains, functionality of the cross-links, etc.) is required.

Networks formed by end-linking processes involving reaction between difunctional polymer chains and a plurifunctional cross-linker are relatively well defined.[1] Once

0024-9297/87/2220-1662$01.50/0

the reaction is complete, the ν precursor chains should have become ν elastically active network chains connected to μ ($=2\nu/f$) cross-links, f being the functionality of the cross-links. Such networks are useful tools to check existing theories. Unfortunately there are always some defects, such as unreacted groups, which lead to the presence of dangling chains. The resulting uncertainty of the actual structural parameters of the networks has affected many earlier works and induced doubt on the conclusions drawn about the validity of the theories tested.

It has been found useful for the investigation of the elastic properties of a network to be coupled with an evaluation of its actual molecular structure. These two theoretical approaches are involved: (a) the theory of gel formation allowing for the determination of the effective parameters of the materials; (b) the theory of the equilibrium elastic response of a collection of ν chains in a network. In this paper, we have focused our attention on these two aspects.

The materials used in this work are formed by reacting α,ω-dihydroxypoly(ethylene oxide) (PEO) with a pluriisocyanate according to a method described recently.[2a] The present study addresses the elastic behavior of PEO networks swollen in dioxane and in water, and we will stay within the limits of small strains.

For each of the networks prepared, the effective structural parameters were evaluated by means of the branching theory; then the properties of these materials were compared with the predictions arising from the various competing theories of rubber elasticity.

Experimental Part

Materials. PEO is commercially available (Hoechst); the molecular weights of the samples used—ranging from 1000 to 10 000g.mol^{-1}—are determined from OH analysis. Their polydispersity, determined by size exclusion chromatography (SEC), is narrow. It was determined that each macromolecule carries two alcohol end groups.[2b]

The pluriisocyanate (Desmodur N 75) is provided by Bayer. It is obtained by a reaction of hexamethylene diisocyanate with water.

$$3O{=}C{=}N(CH_2)_6N{=}C{=}O + H_2O \rightarrow O{=}C{=}N(CH_2)_6NHCOOH \rightarrow O{=}C{=}N(CH_2)_6NH_2 + CO_2$$

$$O{=}C{=}N(CH_2)_6NH_2 + O{=}C{=}N(CH_2)_6N{=}C{=}O \rightarrow O{=}C{=}N(CH_2)_6NHCONH(CH_2)_6N{=}C{=}O$$

$$O{=}C{=}N(CH_2)_6NHCONH(CH_2)_6N{=}C{=}O + O{=}C{=}N(CH_2)_6N{=}C{=}O \rightarrow O{=}C{=}N(CH_2)_6N[CONH(CH_2)_6N{=}C{=}O]_2$$

At this stage, the reaction is not complete. The isocyanate may still react with the biuret formed, leading to species of higher functionality ($f > 3$)

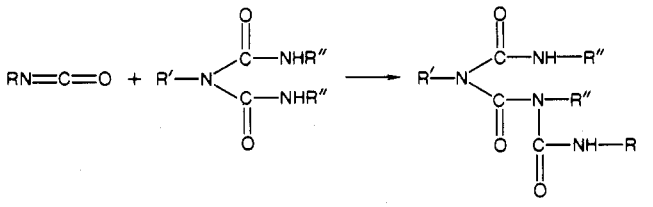

The average functionality evaluated according to a method described previously[2a] is $\bar{f}_w = 6.4$; the distribution of functionalities could be determined by SEC analysis. The SEC diagram shows the existence of at least five different species. The molecular weights of these species were roughly evaluated by SEC calibration with polystyrene (PS) samples, in order to estimate the functionality according to the scheme mentioned above. The amount of each species in the mixture is determined by integrating the peak areas w_i (Table I).

Procedure. The PEO networks are prepared by reaction of α,ω-dihydroxy-PEO with a pluriisocyanate (Desmodur N 75) in stoichiometric amounts and generally in dioxane. The details of the synthesis are described elsewhere.[2] After a fixed reaction time (generally 10–15 days), the gels formed are allowed to swell to equilibrium in an excess of solvent. The soluble fraction is extracted over a 3-week period, the solvent being replaced every second day. To obtain water-swollen gels, a slow solvent exchange is performed.

Table I
Distribution of Functionalities of the Cross-Linking Agent

mass at the peak	w_i	nature of species	f_i	n_i
350	0.024	urea	2	0.055
470	0.33	biuret	3	0.55
850	0.18	double biuret	5	0.17
1500	0.16	triple biuret	7	0.11
>2300	0.3		9	0.115

The networks are characterized by their equilibrium swelling degrees in dioxane and in water and by their elastic moduli arising from uniaxial compression measurements. The equilibrium swelling degree ($Q = 1/v_2$) of the networks is determined according to a method described in previous papers.[3] The equilibrium elastic modulus of swollen samples (after extraction of their soluble constituents) is obtained from uniaxial compression measurements previously described,[2] using the equation $\sigma = E_{G,exp}(\lambda - \lambda^{-2})$, where σ is the stress per unit of cross-sectional area of the sample and λ is the deformation ratio.

Network Formation Theory

The main problem that has plagued the testing of the molecular theories is the uncertainty concerning the network structure. Any relation capable of predicting structural parameters of a gel would be of great interest, once the starting species are given.

Flory[4] was the first to develop a relation giving the critical extent of the reaction p_c to get cross-linking: the gel point is the most important feature in a cross-linking reaction. Later Stockmayer,[5] using combinatorial methods, calculated the distribution of the species formed during the step-growth polymerization. A more recent approach was proposed by Gordon and his co-workers.[6] They showed how the averages of the molecular weight could be estimated by stochastic branching processes and by the probability-generating function. Recently Dusek[7] analyzed epoxy network formation according to this method.

All the theories mentioned above, as well as the cascade model or the statistical combinatorial model, are quite complex and difficult to apply, even to ideal reactions (independent and equal reactivity of functional groups, no loop formation, etc.) To evaluate the extent of reaction and the concentration of effective elastic chains and cross-links, we have utilized the Miller–Macosko theory.[8,9] The treatment put forward by these authors is based on the recursive nature of the branching process and on the elementary probability law. They have derived simple relations between a parameter available experimentally—such as the soluble fraction w_s—and another one characterizing the extent of the reaction (p).

As the calculated concentration of effective elastic chains is based upon the correctness of the network formation theory, its validity has to be checked independently. This has been done by several authors: the good agreement that was found in the pregel region and for the determination of the gel point in systems comparable to ours proves the validity of the branching theory.

Let us consider the network formed by the cross-linking polycondensation of a f_i-functional compound A_{f_i} present at a molar concentration a_{f_i} with a g_i-functional compound B_{g_i}, the molar concentration of which is b_{g_i}. It is assumed that the networks formed are loop-free and that all functional groups are equally reactive and react independently.

Once a fraction p_a of A groups has reacted—in the postgel region—let us pick up an A group at random, take direction 1, and determine which is the probability $P(F_A^{out})$ of finding a finite chain.

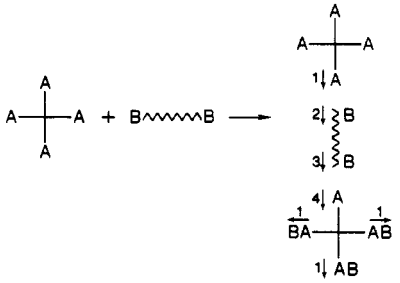

The probability of occurrence of F_A^{out} is governed by p_a. $P(F_A^{out})$ must then be calculated with the law of total probability, taking into account two nonindependent events (F_A^{out}) and the probability of reaction of A with B. Under these conditions

$$P(F_A^0) = P(F_A^0/A_{reacted})P_{A,reacted} + P(F_A^0/A_{unreacted})P_{A,unreacted} \quad (1)$$

If A has reacted, then F_A^0 is equivalent to F_B^{in}, i.e., finding a finite chain when looking into a B unit

$$P(F_A^0) = P(F_B^{in})p_a + (1 - p_a) \quad (2)$$

The B group will be the start of a finite chain if, looking into B from one arm, all other $(g - 1)$ arms are finite; then

$$P(F_B^{in}) = \sum_j b_{g_j}[P(F_B^0)]^{g_j-1} \quad (3)$$

Following direction $\xrightarrow{3}$ we obtain

$$P(F_B^0) = P(F_A^{in})p_b + 1 - p_b \quad (4)$$

$$P(F_A^{in}) = \sum_i a_{f_i}[P(F_A^0)]^{f_i-1} \quad (5)$$

This is a simple recursion, as by combining eq 2–5, one gets

$$p_a\sum_j b_{g_j}[1 - p_b + p_b\sum_i a_{f_i}[P(F_A^0)]^{f_i-1}]^{g_j-1} - P(F_A^0) - p_a + 1 = 0 \quad (6)$$

With the application of these results to our system—polycondensation of a difunctional precursor B with a cross-linking agent containing species of various functionalities $\sum a_{f_i}A_{f_i}$—eq 6 becomes

$$p_a p_b\sum_i a_{f_i}[P(F_a^0)]^{f_i-1} - P(F_A^0) - p_a p_b + 1 = 0 \quad (7)$$

The amount of extractable material (w_s), beyond the gel point, is accessible experimentally. A randomly chosen A or B will be part of the sol fraction if all of their arms lead to finite chains

$$w_s = \sum_i w_{a_{f(i)}}[P(F_A^0)]^{f_i} + w_{b_2}[P(F_B^0)]^2 \quad (8)$$

where $w_{a_{f(i)}}$ is the weight fraction of the A_{f_i}s and w_{b_2} is the weight fraction of B_2s in the initial mixture. To become an active network junction, an A molecule must be connected by at least three "paths" to the gel. The probability of an arm being infinite is $1 - P(F_A^0)$. The probability that a random A molecule is a junction of functionality i is

$$P(x_i) = \binom{f}{i}[1 - P(F_A^0)]^i[P(F_A^0)]^{f-i}, \quad \text{with } i > 3 \quad (9)$$

Since i arms out of f can be infinite, there are $\binom{f}{i}$ possible combinations.

The total concentration of the cross-links is given by the sum of the weighted probabilities of network formation

$$\mu = [A_f]_0 \sum_{i=3}^{f} P(x_i) \quad (10)$$

An elastically active chain is linked at both ends to active cross-links (junctions). It follows that

$$\nu = [A_f]_0 \sum_{i=3}^{f} (i/2)P(x_i) \quad (11)$$

Results and Discussion. The relations given up to this point allow for the calculation of the effective parameters (ν, μ) of the gels, knowing the soluble (extractable) fraction w_s. But prior to the use of the branching theory, it is important to check whether the assumptions made—such as equal and independent reactivity and no loop formation—are valid for our system. For that purpose, we have used a linear model and investigated the step growth polymerization of OH-terminated PEO with a bifunctional isocyanate.[2b] Chain extension reactions performed under the same conditions as the network formation reactions (temperature, stoichiometric balance, concentration) are free of cycle formation, and no side reaction (allophanate) has been detected. As the chemical requirements are met, one can consider the Miller–Macosko approach as suitable to describe the PEO network formation (even though the theory has not been tested independently).

As mentioned in the Experimental Part, the cross-linking agent is a mixture of species with different functionalities; eq 7 may be written as

$$p^2(a_2P(F_A^0) + a_3[P(F_A^0)]^2 + a_5[P(F_A^0)]^4 + a_7[P(F_A^0)]^6) - P(F_A^0) - p^2 + 1 = 0 \quad (12)$$

For our particular system the first term of eq 8 is negligible with respect to the second. The soluble fraction is therefore simply

$$w_s = [P(F_B^0)]^2 \quad (13)$$

As $P(F_A^0)$ is related to $P(F_B^0)$ by

$$P(F_A^0) = p[P(F_B^0) - 1] + 1$$

eq 12 becomes

$$p^2[a_7[p(P(F_B^0) - 1) + 1]^6 + a_5[p(P(F_B^0) - 1) + 1]^4 + a_3[p(P(F_B^0) - 1) + 1]^2 + a_2[p(P(F_B^0) - 1) + 1]] - p(P(F_B^0) - 1) - p^2 + 1 = 0 \quad (14)$$

The knowledge of w_s—soluble fraction— gives access to the extent of the reaction p. Equation 14 is solved by computer. To calculate other structural parameters (ν,μ), we have used expressions 10 and 11.

In Table II are listed the characteristics of three series of gels prepared from five different PEO samples. For each series, v_{2c}, the volume fraction of polymer during the cross-linking process, has been chosen to be almost identical.

Tables III and IV display the data on gels obtained from the same precursor (successively M_n = 1800 and M_n = 5600) but cross-linked at different polymer volume fractions v_{2c}.

The influence of the duration of reaction is evidenced in Table V. Reaction times range from 20 to 168 h under identical conditions (same M_n of precursor, same v_{2c}).

From the data displayed in Tables II–V, one can make two observations:

a. The maximum conversion attained is about 0.95. This indicates that the reaction goes nearly to completion but never totally, even after 10 days of reaction.

b. The greatest values of p are obtained for the gels prepared in the bulk or at high concentrations. In other words, when the initial polymer fraction is rather low ($v_{2c} \leq 0.2$), the amount of soluble material is larger, which may be attributed to lower conversion rates and/or to cyclizations.

Table II
Structural Parameters of Three Series of PEO Gels Prepared from Five Different PEO "Precursors"

M_n[a]	w_s,[b] %	v_{2c}[c]	p[d]	$[\nu]_0$,[e] mol L^{-1}	$[A_f]_0$,[f] mol L^{-1}	$[\nu]$,[g] mol L^{-1}	$[\mu]$,[h] mol L^{-1}
1010	2.1	0.24	0.893	0.186	0.088	0.114	0.055
1810	2.1	0.22	0.893	0.108	0.051	0.066	0.032
3400	5.3	0.2	0.843	0.059	0.028	0.027	0.014
5600	5.2	0.19	0.845	0.036	0.017	0.017	0.008
8300	3.4	0.18	0.87	0.025	0.012	0.014	0.007
1010	2.4	0.4	0.88	0.298	0.141	0.175	0.085
1810	1.3	0.35	0.914	0.178	0.084	0.12	0.057
3400	1.5	0.33	0.908	0.098	0.046	0.065	0.031
5600	2.2	0.32	0.892	0.060	0.028	0.036	0.017
8300	5.1	0.31	0.847	0.041	0.019	0.02	0.01
1010	1.6	0.56	0.905	0.425	0.201	0.276	0.132
1810	0.5	0.53	0.944	0.262	0.124	0.196	0.088
3400	1.7	0.5	0.903	0.148	0.07	0.095	0.046
5600	1.8	0.48	0.9	0.092	0.043	0.058	0.028
8300	1.3	0.47	0.913	0.063	0.03	0.043	0.021

[a] M_n is the average molecular weight of the PEO "precursor". [b] w_s is the sol fraction. [c] v_{2c} is the volume fraction of polymer segment upon cross-linking. [d] p is the extent of the reaction. [e] $[\nu]_0$ is the initial concentration of the PEO chains. [f] $[A_f]_0$ is the initial concentration of the cross-linking agent. [g] $[\nu]$ is the concentration of the elastically effective PEO network chains (eq 10). [h] $[\mu]$ is the concentration of the network junctions (eq 11).

Table III
Structural Characteristics of the Networks: Influence of the Volume Fraction of Polymer Segments upon Cross-Linking, v_{2c} (Polymer "Precursor" M_n = 1800)

w_s, %	v_{2c}	p	$[\nu]_0$, mol L^{-1}	$[A_f]_0$, mol L^{-1}	$[\nu]$, mol L^{-1}	$[\mu]$, mol L^{-1}
21	0.055	0.734	0.027	0.013	0.006	0.004
14	0.077	0.771	0.038	0.018	0.012	0.007
1.8	0.11	0.9	0.055	0.026	0.033	0.017
1	0.16	0.923	0.081	0.038	0.057	0.027
2.1	0.22	0.894	0.108	0.051	0.066	0.032
1.3	0.356	0.913	0.178	0.084	0.12	0.057
0.5	0.525	0.944	0.262	0.124	0.196	0.088
1.3	0.612	0.913	0.305	0.144	0.258	0.113
0.3	1	0.955	0.497	0.235	0.386	0.182

Table IV
Structural Characteristics of the Networks: Influence of the Volume Fraction of the Polymer Segment v_{2c} upon Cross-Linking (Polymer "Precursor" M_n = 5600)

w_s, %	v_{2c}	p	$[\nu]_0$, mol L^{-1}	$[A_f]_0$, mol L^{-1}	$[\nu]$, mol L^{-1}	$[\mu]$, mol L^{-1}
5.21	0.19	0.85	0.036	0.017	0.017	0.008
2.2	0.32	0.89	0.060	0.028	0.036	0.017
1.82	0.48	0.9	0.092	0.043	0.058	0.028
0.97	0.57	0.924	0.109	0.051	0.078	0.037
0.2	1	0.96	0.198	0.09	0.161	0.075

Table V
Structural Characteristics of the Networks: Influence of the Duration of Reaction t (Polymer "Precursor" M_n = 5600)

t,[a] h	w_s, %	v_{2c}	p	$[\nu]_0$, mol L^{-1}	$[A_f]_0$, mol L^{-1}	$[\nu]$, mol L^{-1}	$[\mu]$, mol L^{-1}
20	35.4	0.32	0.679	0.06	0.028	0.0042	0.002
31	30.6	0.32	0.695	0.06	0.028	0.0057	0.003
55	16.5	0.32	0.756	0.06	0.028	0.014	0.007
79	11.5	0.32	0.796	0.06	0.028	0.021	0.01
103	7.5	0.32	0.821	0.06	0.028	0.027	0.013
168	2.2	0.32	0.892	0.06	0.028	0.042	0.019

[a] t is the duration of the reaction.

Theories of Rubber Elasticity

Models. Affine Networks. The main aim of the rubber elasticity theories is to establish relationships between a macroscopic strain and the resulting conformational changes in the network chains. Originally it was assumed that the position of the network junctions were affine[10] with respect to macroscopic strain, implying the same effect on the end-to-end vectors.

The free energy of a single chain is related to its displacement; it follows from the assumption introduced above that the total free energy of the network is the sum of the contributions of all individual strands. If one takes into account the term $\mu RT \ln V$ for the dispersion of the junctions over the volume V and expresses the free energy with respect to the reference state V^0, one gets

$$\Delta A = (\nu/2)RT(\lambda_x^2 + \lambda_y^2 + \lambda_z^2 - 3) - \mu RT \ln (V/V^0) \quad (15)$$

The modulus is obtained by derivation of eq 15

$$E_{G,affine} = \frac{\sigma}{\lambda - \lambda^{-2}} = \nu RT \quad (16)$$

where $\sigma = F/A$ is the nominal stress, F the elastic force, and A the cross-sectional area of the sample.

"Phantom" Networks. In a second approach,[11] the network chains are assumed to be "phantom"; they are

Table VI
Experimental and Theoretical Elastic Moduli Calculated with the "Phantom" and "Affine" Network Theories: Influence of the Average Molecular Weight of the PEO "Precursor"

M_n	w_s, %	v_{2c}	v_2[a]	ν, mol L^{-1}	$\nu - \mu$,[b] mol L^{-1}	$10^{-5}E_{G,phantom}$[c]	$10^{-5}E_{G,affine}$[c]	$10^{-5}E_{G,expt}$[d]
1010	2.1	0.24	0.133	0.114	0.059	11.44	22.1	6.14
1810	2.1	0.22	0.121	0.066	0.034	6.74	13	
3400	5.3	0.2	0.047	0.027	0.013	1.9	4.03	1.65
5600	5.2	0.19	0.043	0.017	0.008	1.2	2.46	1.01
8300	3.4	0.18	0.04	0.013	0.007	0.98	1.93	1.05
1010	2.4	0.4	0.177	0.175	0.090	16.4	32	17.2
1810	1.3	0.35	0.129	0.12	0.063	10.8	20.5	11.6
3400	1.5	0.33	0.075	0.065	0.034	4.97	9.55	5.07
5600	2.2	0.32	0.077	0.036	0.018	2.76	5.36	4.32
8300	5.1	0.31	0.063	0.020	0.010	2.28	4.5	3.25
1010	1.6	0.56	0.207	0.276	0.144	23.8	46.8	22
1810	0.5	0.53	0.189	0.196	0.108	18.4	33.5	26.5
3400	1.7	0.5	0.106	0.095	0.049	7.09	13.6	7.87
5600	1.8	0.48	0.096	0.058	0.03	4.24	8.17	6.14
8300	1.3	0.47	0.077	0.043	0.022	2.95	5.65	5.2

[a] v_2 is the volume fraction of the polymer segment at the swelling equilibrium ($=Q^{-1}$) [b] $\nu - \mu$ is the cycle rank according to Flory.[15] [c] $E_{G,phantom}$ and $E_{G,affine}$ (in dyn/cm^2) are calculated according to eq 19 and 20, respectively. [d] $E_{G,expt}$ is the experimental elastic modulus (in dyn/cm^2).

"immaterial" and can cross each other freely. Their only role is to exert forces on the junctions. Being free of constraints, the junctions can fluctuate (Δr) independently of the stress.

As a matter of fact, the actual chain vector distribution is the convolution of the mean chain vector distribution with the fluctuation distribution. It is not affine with respect to the strain. This theory leads to an elastic free energy similar to the previous one but with a smaller coefficient[12]

$$E_{G,phantom} = (\nu - \mu)RT \quad (17)$$

It was shown that the difference $\nu - \mu$ is the cycle rank ξ, in other terms the number of network chains that have to be cut to dismantle the network into an ensemble of star molecules.

Deformation of a Swollen Network. Relations 16 and 17 address the elastic behavior of dry networks. Flory[13] has derived the expressions for the modulus of a gel, swollen to equilibrium, according to the affine model

$$E_{G,affine} = RT(\nu/V_0)v_2^{1/3} \quad (18)$$

Here ν/V_0 is the number of elastically effective chains per unit volume of dry network, since ν is the number of elastic chains in the volume V_0 of network formed supposedly in the bulk; v_2 is the volume fraction of network in the swollen state (i.e., the reciprocal of Q).

If the cross-linking reaction is not carried out in the dry state, one has to take into account the polymer volume fraction v_{2c} in the "nascent" state. Equation 18 becomes

$$E_{G,affine} = RT(\nu/V_0)v_{2c}^{-1/3}v_2^{1/3} \quad (19)$$

$\nu/V_0 = \nu_e$ is the number of elastic chains per unit volume in the "nascent" state.

Extending this expression to the "phantom" case, one would obtain

$$E_{G,phantom} = RT(\nu_e - \mu_e)v_{2c}^{-1/3}v_2^{1/3} \quad (20)$$

Results and Discussion

PEO Networks Swollen to Equilibrium in Dioxane. The experimental determination of the elastic moduli is performed in the swollen state within the limit of small strains. Our aim is to establish the influence of parameters such as the length of the elastic chains (characterized by M_n) or the concentration at which the cross-linking process takes place (characterized by the volume fraction v_{2c}) on the mechanical behavior and to evaluate the ability of each of the competing theories to account for the results. Since the effective parameters of the network structure can be easily calculated—using the branching theory—it is possible to predict the behavior of the PEO gels according to the "affine" and "phantom" models. The swelling ratio being determined in each case, expressions 19 and 20 lead to the theoretical elastic moduli $E_{G,affine}$ and $E_{G,phantom}$. These values and the experimental results, obtained by compression on swollen samples, are listed in Table VI.

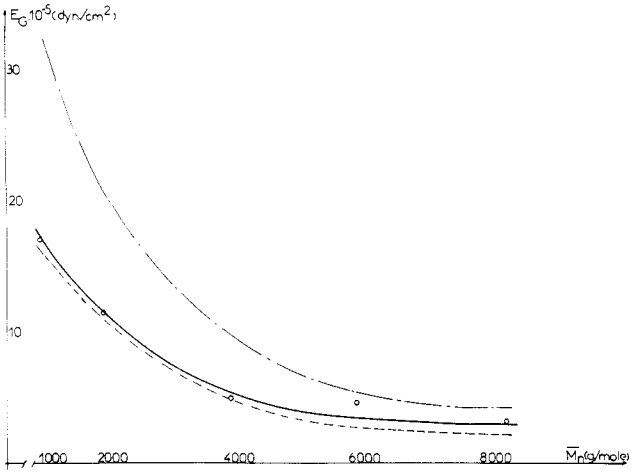

Figure 1. Dependence of the modulus (E_G) on the length of the elastic chains: (—) curve drawn from experimental data; (-·-) curve calculated according to the "affine" model; (---) curve calculated according to the "phantom" model.

Influence of the Length of the Elastic Chains. Experimental and theoretical moduli are plotted vs. the molecular weight of the elastic chains for a series of swollen networks prepared at almost the same polymer volume fraction, v_{2c}, in Figure 1. Figure 2 displays the same moduli as a function of the polymer volume fraction v_2 corresponding to the respective equilibrium swelling degrees.

From both representations it appears that the experimental behavior of the networks is intermediate between the "affine" and "phantom" models.

For the networks exhibiting the longest PEO chains the values of the moduli arising from the "phantom" model are underestimated. In this case the "affine" model appears to be a satisfactory approximation. For the networks cross-linked at lower concentrations ($v_{2c} \simeq 0.2$), the

Table VII
Experimental and Theoretical Elastic Moduli Calculated with the "Phantom" and "Affine" Network Theories: Influence of v_{2c} (Polymer "Precursor" M_n = 1810)

w_s, %	v_{2c}	v_2	ν, mol L^{-1}	$\nu - \mu$, mol L^{-1}	$10^{-5}E_{G,phantom}$	$10^{-5}E_{G,affine}$	$10^{-5}E_{G,expt}$
21	0.055	0.027	0.006	0.002	0.4	1.17	0.2
14	0.077	0.039	0.012	0.005	0.98	2.25	0.7
1.8	0.11	0.08	0.033	0.016	3.57	7.23	3.38
1	0.16	0.095	0.057	0.030	6	11.4	7.05
2.1	0.22	0.121					
1.3	0.356	0.129	0.12	0.063	10.68	20.5	11.6
0.5	0.525	0.189	0.196	0.107	18.4	33.5	26.5
1.3	0.612	0.214	0.258	0.135	22.8	43.7	32.1
0.3	1	0.254	0.386	0.204	31	58.7	45

Table VIII
Experimental and Theoretical Moduli Calculated with the "Phantom" and the "Affine" Network Theories: Influence of the Polymer Volume Fraction v_{2c} upon Cross-Linking (Polymer "Precursor" M_n = 5600)

w_s, %	v_{2c}	v_2	ν, mol L^{-1}	$\nu - \mu$, mol L^{-1}	$10^{-5}E_{G,phantom}$	$10^{-5}E_{G,affine}$	$10^{-5}E_{G,expt}$
5.2	0.19	0.043	0.017	0.0083	1.2	2.46	1.01
2.2	0.32	0.078	0.036	0.018	2.76	5.36	4.32
1.82	0.48	0.096	0.058	0.030	4.24	8.17	6.14
0.97	0.57	0.130	0.078	0.041	5.94	11.4	14.1
0.2	1	0.214	0.161	0.086	12.4	23.1	29.6

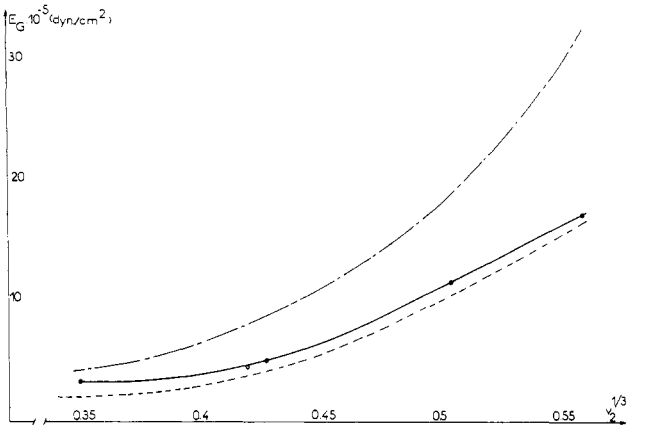

Figure 2. Modulus (E_G) as a function of the polymer volume fraction (v_2) for networks prepared at almost the same polymer volume fraction in the "nascent" state (v_{2c}): (—) curve drawn from experimental data; (-·-) curve calculated according to the "affine" model; (---) curve calculated according to the "phantom" model.

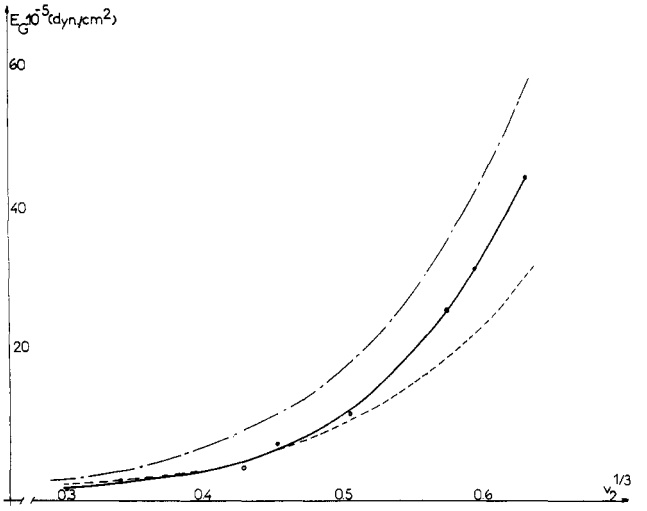

Figure 3. Modulus (E_G) as a function of the polymer volume fraction (v_2) for networks prepared from a same precursor (M_n = 1810) but at different v_{2c}s ranging from 0.05 to 1: (—) curve drawn from experimental data; (-·-) curve calculated according to the "affine" model; (---) curve calculated according to the "phantom" model.

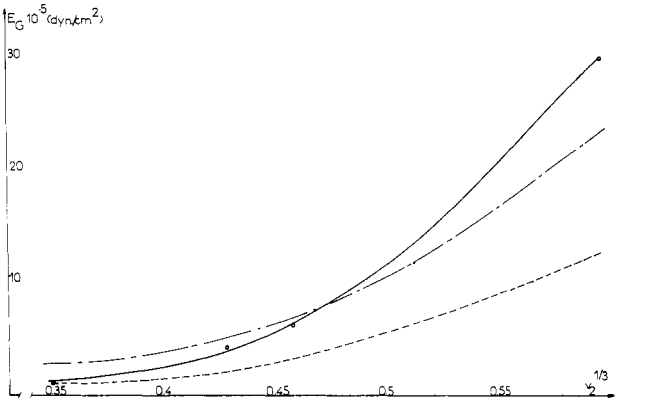

Figure 4. Modulus (E_G) as a function of the polymer volume fraction (v_2) for networks prepared from a same precursor (M_n = 5600) but at different v_{2c}s ranging from 0.18 to 1: (—) curve drawn from experimental data; (-·-) curve calculated according to the "affine" model; (---) curve calculated according to the "phantom" model.

agreement between "phantom" behavior and experimental observations appears to be satisfactory.

Influence of the Concentration (Volume Fraction v_{2c}) at Which Cross-Linking Took Place. Networks prepared from the same precursor exhibit quite different properties at swelling equilibrium, depending upon the concentration of the precursor solution. To understand the effect of the "nascent" polymer fraction (by volume) v_{2c}, we have prepared a set of five gels starting from the same precursor PEO (M_n = 1800) cross-linked at v_{2c}s ranging from 0.05 to 1. The experimental values of the elastic moduli are listed in Table VII along with the theoretical values predicted with "phantom" and "affine" models, respectively. At higher "initial" concentrations (v_{2c}), the moduli observed will be higher. Experimental values agree with those originating from the "phantom" model when v_{2c} is rather low. As v_{2c} increases, the experimental moduli are located between the "phantom" and "affine" limits (Figure 3). The same procedure has been applied to another PEO (M_n = 5600), v_{2c} ranging in this case from 0.18 to 1. From Table VIII and Figure 4, the same behavior is seen as in the former case. When v_{2c} is low, the "phantom" model is a good approach. At intermediate concentrations, $0.3 < v_{2c} < 0.5$, the experimental

moduli are close to those expected from the "affine" model. At high concentrations or in the bulk, ($v_{2c} > 0.9$) the values of the moduli predicted on the basis of both models are underestimated.

Contribution of Entanglements. As shown before, the experimental studies on PEO networks indicate systematic departures from the predictions of the classical theories. The behavior of real networks is generally intermediate between the two models—"affine" and "phantom".

Several authors have reconsidered the theories of rubber elasticity to take into account the following ideas:

a. There is no "affine" relationship between the macroscopic strain and the chain vector distribution.

b. Network chains are no "phantoms". They cannot freely cross each other, though they do interpenetrate.

A qualitative model has been proposed by Bastide et al.[14] According to these authors, large macroscopic deformations involve topological reorganization of spatial neighbors, through partial "disinterpenetration" of the chains, inducing for each of them only small deformations. Conversely, the highly cross-linked gels (or those constituted of short chains) should behave in an "affine" manner.

Another—more quantitative—approach based upon the "phantom" model has been put forward by Flory.[15a] He suggested that interactions between chains can be expressed in terms of a limitation of the fluctuations of the junctions around their average position. Departure from the "phantom" model should occur to an extent that is a function of strain: at small deformations the entanglements restrain the junction fluctuations, which implies an increase of the modulus relative to that exhibited by a "phantom" network. At larger strains, owing to the partial disentanglement of the chains, the interactions become less effective and can even vanish. One tends then toward the "phantom" behavior.

The energy function derived by Flory[15b] involves two parameters: κ and ξ. κ is a measure of the severity of the constraints imposed by neighboring chains on the network junctions. It is entirely determined by the chemical structure of the network. ($\kappa \to 0$ corresponds to the "phantom" network; $\kappa \to \infty$, if junction fluctuations are entirely suppressed, occurs in the "affine" model.)

The other parameter ξ takes into account the variation of the distribution function of network chains, along with the deformation. ξ is not fully determined by the network structure.

For small strains (with $\xi = 0$), Flory's model predicts, depending upon the value of κ

$$(\nu - \mu)RT \leq E_G \leq \nu RT \tag{21}$$

The left term holds for $\kappa = 0$ and the right term for $\kappa \to \infty$.

The theory of Dossin and Graessley[16] is similar to Flory's approach, but it is valid only for small strains. An empirical parameter h is introduced to measure the magnitude of the constraints on "junction fluctuations"; h can vary between 0 (complete suppression) and 1 ("phantom" network). However, contrary to Flory, who considered the topological interactions as restricting the junction fluctuations, Graessley estimated that under small strains the chain–chain interactions may also act as additional cross-links (entanglements). This originates from the fact that linear high MW polymers behave in dynamic mechanical tests as if they were cross-linked. Graessley therefore introduced an additional term, $G_n T_e$, into the expression of the modulus; T_e represents the fraction of topological interactions permanently trapped (during the cross-linking process). G_n is the plateau modulus of the linear homologue of the network

$$E_G = (\nu - h\mu)RT + T_e G_n \tag{22}$$

Numerous other theories have been recently put forward to account for entanglements in polymer networks. These models can be classified in three categories:[18]

a. In the tube models[19,20] each chain is assumed to be confined within a tube.

b. In the slip-link model[21,22], the chain creeps through small rings which represent the entanglements. The portion of chain comprised between two consecutive slip-links is adjustable.

c. In the "primitive path" model[23,24] the network chain comprises two types of segments: those belonging to the "primitive path", located in the direct line between chain ends, and those in excess, lying outside the "primitive paths".

As the end-to-end distance of the elastic chains lengthens during the deformation, the "excess" segments are gradually transferred into the "primitive path".

We have not tested the ability of the theories mentioned above to describe the behavior of our PEO networks. We have focused our attention on the constrained junction fluctuation model as it rests on reasonable physical concepts and provides for simple mathematical expressions. The interpretation proposed for our data on small strain moduli combines Flory's junction suppression model with Langley's trapped entanglements concept. It turns out indeed that Flory's theory alone cannot model our experimental results. In a few cases, the upper limit νRT (eq 21) originating from Flory's analysis is lower than the modulus measured (Table VIII, Figure 4). This clearly indicates that the entanglements not only are limiting the junction fluctuations but also may be considered as additional cross-links.

This analysis leads to the following expression for the modulus:

$$E_G = [(\nu - h\mu) + T_e\epsilon(2 - h)]RT v_2^{1/3} v_{2c}^{-1/3} \tag{23}$$

Here h is an empirical parameter first introduced by Dossin and Graessley[16] which varies between 0 and 1. It depends upon the swelling degree Q of the sample ($1/v_2$); for highly swollen networks h should tend toward 1. ϵ is a function of both the precursor molecular weight and the polymer volume fraction v_{2c} upon cross-linking. According to Ferry,[24] the molecular weight between two entanglements M_{en} for linear PEO in the bulk is $M_{en} = 2200$; this implies that entanglements should appear only in networks made of elastic chains with molecular weights higher than 4400. T_e, the trapping factor, is defined in terms of the Macosko–Miller theory as the probability for the four arms of two chains leading away from an entanglement to go to infinity. In our system, the functionality of the entanglements should be predominantly 4. Thus

$$T_e = (1 - P(F_B^0))^4 \tag{24}$$

Interpretation of Results. Gels Involving a Short Chain ($M_n < 2000$). We have commented above upon the influence of the polymer volume fraction in the "nascent" state (v_{2c}) on the behavior of our PEO gels. The difference between the "phantom" predictions and the experimental results may only arise from the limitations of junction fluctuations. As the chains are short the entanglements can be disregarded. Equation 23 can be written as

$$E_G = RT(\nu - h\mu)v_2^{1/3} v_{2c}^{-1/3} \tag{25}$$

Depending upon the concentration v_{2c} while the polymer is cross-linking, the fluctuations of the junctions would be hindered more or less. Knowing ν and μ, the experimental

Table IX
Evaluation of the Empirical Parameter h for Networks Prepared from Short PEO Chains (M_n = 1810)

v_{2c}	v_2	ν, mol L^{-1}	μ, mol L^{-1}	$10^{-5}E_{G,expt}$	$E_{G,expt}/(RTv_2^{1/3}u_{2c}^{-1/3})$	h[a]
0.055	0.027	0.006	0.004	0.2	0.001	
0.077	0.039	0.012	0.007	0.7	0.004	1
0.11	0.08	0.033	0.017	3.38	0.016	1
0.16	0.095	0.057	0.027	7.05	0.035	0.82
0.22	0.121					
0.356	0.129	0.12	0.057	11.6	0.067	0.9
0.525	0.189	0.196	0.088	26.5	0.155	0.46
0.612	0.214	0.258	0.113	32.1	0.189	0.45
1	0.254	0.386	0.182	45	0.295	0.49

[a] h is an empirical parameter calculated according to eq 25

$$E_G = RT(\nu - h\mu)v_2^{1/3}v_{2c}^{-1/3} \tag{25}$$

Table X
Evaluation of the Entanglement Concentration ϵ for PEO Networks Prepared at Different v_{2c} Values, from Long PEO Chains

M_n = 5600							
v_{2c}	v_2	ν, mol L^{-1}	μ, mol L^{-1}	h	Te[a]	$10^{-5}E_{G,expt}$	ϵ,[b] mol L^{-1}
0.19	0.043	0.017	0.008	1	0.355	1.01	0
0.32	0.078	0.036	0.017	1	0.526	4.32	0.01
0.48	0.096	0.058	0.026	0.9	0.562	6.14	0.026
0.57	0.13	0.078	0.037	0.8	0.663	14.1	0.04
1	0.214	0.161	0.075	0.45	0.83	29.6	0.061

[a] Te = $[1 - (P_B^0)]^4$. [b] ϵ is determined by the following equation:

$$\epsilon = \left[\frac{E_{G,expt}v_2^{-1/3}v_{2c}^{1/3}}{RT} - \nu + h\mu\right]\frac{1}{\mathrm{Te}(2-\mathrm{h})}$$

Table XI
Characteristics of PEO Networks Exhibiting Short Elastic Chains (M_n < 2000) Swollen at Equilibrium in Water

M_n	v_{2c}	v_2	ν, mol L^{-1}	$\nu - \mu$, mol L^{-1}	$10^{-5}E_{G,phantom}$	$10^{-5}E_{G,affine}$	$10^{-5}E_{G,expt}$
1810	0.055	0.033	0.006	0.002	0.43	1.25	0.24
1810	0.077	0.049	0.012	0.005	1.05	2.4	0.53
1810	0.11	0.093	0.033	0.016	3.73	7.5	4.25
1810	0.16	0.116	0.057	0.03	6.44	12.25	7.84
1010	0.4	0.230	0.175	0.09	17.9	35	19.8
1810	0.356	0.152	0.12	0.063	11.3	21.5	12.7
1010	0.56	0.254	0.276	0.144	25.5	50.2	24.9
1810	0.525	0.201	0.196	0.108	18.78	34.2	23.3
1810	0.612	0.220	0.258	0.135	23	43.8	35.5
1810	1	0.259	0.336	0.204	31.12	59	46.4

Table XII
Characteristics of PEO Networks Exhibiting Long Elastic Chains (M_n > 4000) Swollen at Equilibrium in Water

M_n	v_{2c}	v_2	ν, mol L^{-1}	$\nu - \mu$, mol L^{-1}	$10^{-5}E_{G,phantom}$	$10^{-5}E_{G,affine}$	$10^{-5}E_{G,expt}$
8300	0.18	0.0267	0.013	0.007	0.85	1.68	0.2
5600	0.19	0.0275	0.017	0.008	1.03	2.11	0.25
3400	0.2	0.0288	0.027	0.013	1.61	3.42	0.38
8300	0.31	0.049	0.02	0.01	2.07	4.08	2.56
5600	0.32	0.064	0.036	0.018	2.61	5.07	2.15
3400	0.33	0.066	0.065	0.034	4.76	9.15	2.98
8300	0.47	0.036	0.043	0.022	2.26	4.33	0.64
5600	0.48	0.075	0.058	0.03	3.91	7.55	3.45
3400	0.5	0.096	0.095	0.049	6.89	13.22	6.38
5600	0.57	0.081	0.078	0.041	5.13	9.85	6.66
5600	1	0.21	0.161	0.086	12.3	22.9	37.6

determinations of E_G and v_2 allow us to calculate h. It is confirmed that the samples with low values of v_{2c} and v_2 are those for which the values of h are the highest. For our samples with short PEO chains, h varies from 0.45 (for $v_2 \simeq 0.2$) to 1 (for $v_2 < 0.07$) (Table IX).

Gels Involving Long Elastic Chains (M_n > 4000). In this case, both the limitation of junction fluctuations and the contribution of entanglements are to be taken into account. As previously, all the parameters of eq 23 are known or determined experimentally, except h and ϵ. It can be assumed that the h parameter is the same for gels exhibiting the same swelling ratio, as h is specific for a given v_2. The estimated value of h originating from networks involving short chains allows us thus to calculate ϵ. Table X shows the marked dependance of ϵ on v_{2c}. For higher values of v_{2c}, ϵ is higher. Furthermore, the value of ϵ in PEO cross-linked in the bulk corroborates the measurements of Ferry carried out on linear PEO (which led to M_{en} = 2200).

PEO Networks Swollen in Water. We have also characterized PEO gels swollen to equilibrium in water according to the procedure described above. There are slight differences with the data obtained in dioxane owing to the hydrophobic nature of the cross-linking agent. The

Table XIII
Determination of the Flory–Huggins Interaction Parameter χ (Dioxane–PEO Network)

M_n	v_{2c}	v_2	$E_{G_{expt}}/(RT{v_2}^{1/3}{v_{2c}}^{-1/3})$	χ^a
1800	0.054	0.027	0.001	0.34
1800	0.076	0.039	0.004	(0.405)
1800	0.109	0.08	0.015	(0.405)
1800	0.162	0.095	0.035	0.347
1800	0.356	0.129	0.067	0.354
1800	0.525	0.189	0.154	0.375
1800	0.612	0.214	0.189	0.39
1800	1	0.254	0.295	0.405
5600	0.181	0.043	0.007	0.356
5600	0.315	0.078	0.028	(0.308)
5600	0.48	0.095	0.044	0.334
5600	0.57	0.130	0.096	(0.305)
5600	1	0.214	0.205	0.39

[a] χ is Flory–Huggins interaction parameter dioxane–PEO network calculated according to relation 27.

short-chain PEO gels exhibit in water swelling ratios ($Q = 1/v_2$) lower than those measured in dioxane (Table XI). Conversely, the networks with large elastic chains swell more in water than in dioxane (Table XII).

Nevertheless an interpretation similar to that presented above for dioxane swollen gels can be proposed. In the case of short-chain gels, the deviation from the "phantom" behavior may be attributed solely to the limitations of junction fluctuations. For the networks with large chains both the constraints on junction fluctuations and the trapped entanglements have to be considered to explain the observed departure.

Some results remain unexplained. A few gels prepared at high dilution exhibit—once swollen in water—elastic moduli lower even than those predicted by the "phantom" theory.

This behavior could originate from associations between hydrophobic network junctions, whereby the number of elastically effective network chains is reduced. It should be kept in mind, however, that networks prepared at high dilution have generally reached conversions lower than those obtained in concentrated media. The number of elastically effective chains is thus reduced.

χ Parameter Determination

Flory[4] has related the cycle rank $\xi = \nu - \mu$ of a "phantom" network with the equilibrium swelling degree $Q = 1/v_2$ as

$$\nu - \mu = \frac{\ln (1 - v_2) + v_2 + {v_2}^2\chi}{\bar{V}_1[(v_2/v_{2c})^{1/3} - (\mu/\nu)(v_2/v_{2c})]} \quad (26)$$

As the PEO networks do not behave as "phantom" gels, it is preferable to replace $\xi = \nu - \mu$ by $E_{G,ex}(RT{v_2}^{1/3}{v_{2c}}^{-1/3})^{-1}$ Relation 26 then becomes

$$\frac{E_{G,exp}}{RT({v_2}^{1/3}{v_{2c}}^{-1/3})} = \frac{\ln (1 - v_2) + v_2 + {v_2}^2\chi}{\bar{V}_1[(v_2/v_{2c})^{1/3} - (\mu/\nu)(v_2/v_{2c})]} \quad (27)$$

Table XIII gathers the values of χ calculated for gels swollen in dioxane, according to relation 27. It is confirmed that the values of χ (interaction parameter between gel and solvent) decreases as the swelling degree increases. Dioxane turns out to be a good solvent for elastic chains and for cross-links.

The case of PEO gels swollen in water is markedly different, as the urethane links formed upon cross-linking are hydrophobic, as mentioned before. This is clearly evidenced by the higher values of χ (Table XIV) obtained, showing that water as a swelling solvent is worse than dioxane. χ evidently depends upon the proportion of the hydrophobic agent (Desmodur N 75) necessary to achieve cross-linking. Gels involving long PEO chains and containing therefore a lower proportion of urethane exhibit χ values that are close (0.45) to that given by literature[26] for linear PEO. This can be considered as a check of the validity of our calculation.

Table XIV
Determination of the Flory–Huggins Interaction Parameter χ (Water–PEO Network)

M_n	v_{2c}	v_2	$E_{G,expt}/({v_2}^{1/3}{v_{2c}}^{-1/3}RT)$	χ^a
1800	0.055	0.033	0.0012	0.478
1800	0.076	0.049	0.002	0.48
1800	0.109	0.094	0.018	0.505
1800	0.162	0.117	0.036	0.579
1800	0.216	0.139	0.52	0.53
1800	0.356	0.152	0.070	0.5257
1800	0.525	0.202	0.133	0.546
1800	0.612	0.22	0.207	0.545
1800	1	0.259	0.302	0.566
5600	0.181	0.027	0.002	0.481
5600	0.315	0.064	0.015	0.489
5600	0.48	0.075	0.026	0.487
5600	0.57	0.08	0.053	0.462
5600	1	0.209	0.263	0.529
8300	0.308	0.05	0.002	0.45
8300	0.471	0.035	0.006	0.47

[a] χ is the Flory–Huggins interaction parameter water–PEO network calculated according to relation 27.

Conclusion

The swelling and deformation behavior of a number of poly(ethylene oxide) (PEO) model networks, obtained by end-linking, at various concentrations, and starting from PEO precursors of various molecular weights, has been investigated systematically. As a network is never perfect, it was of great importance to evaluate the *real* number of elastically effective network chains ν and junctions μ. This was done by means of Miller–Macosko branching theories, starting from the amount of extractable material.

The stress–strain behavior of these PEO networks, swollen either in dioxane or in water, cannot be fitted adequately by the "affine" model or by the "phantom" model. It has been therefore the purpose of this work to suggest a reformulation of Flory's theory, taking into account the contribution of trapped entanglements and the limitation of the fluctuations of the junction positions to the elastic modulus. Combination of Flory's basic ideas with the small-strain theory of Langley and Graessley gives a satisfactory fit of theoretical expectation with experimental results. It was established that entanglements play a role when the elastic chains are relatively long, whereas the limitation of junction fluctuations has to be considered for networks exhibiting short chains. It is however necessary to be aware that the corrections introduced into Flory's theory involve two additional adjustable parameters, T_e, the trapping factor, and h, characterizing the constraints on junction fluctuations, both first introduced by Graessley.

Registry No. (PEO)(Desmodur N 75) (copolymer), 88842-45-9.

References and Notes

(1) Rempp, P.; Herz, J. E.; Borchard, W. *Adv. Polym. Sci.* **1978**, *26*, 105.
(2) (a) Gnanou, Y.; Hild, G.; Rempp, P. *Macromolecules* **1984**, *17*, 945. (b) Gnanou, Y.; Chaumont, Ph.; Lutz, P.; Hild, G.; Rempp, P. *Makromol. Chem.* **1984**, *185*, 2647.
(3) Hild G. *Makromol. Chem.* **1976**, *177*, 1947.
(4) Flory, P. J. *Principles of Polymer Chemistry*; Cornell University Press: Ithaca, NY 1953; Chapter 9; *J. Am. Chem. Soc.* **1941**, *63*, 3083.
(5) Stockmayer, W. H. *J. Chem. Phys.* **1943**, *11*, 45; **1944**, *12*, 125.

(6) Gordon, M. *Proc. R. Soc. London, A* **1962**, *268*, 240.
(7) Dusek, K.; Ilavsky, M.; Lunak, S. *J. Polym. Sci., Polym. Symp.* **1975**, *53*, 29.
(8) Macosko, C. W.; Miller, D. R. *Macromolecules* **1976**, *9*, 199.
(9) Miller, D. R.; Macosko, C. W. *Macromolecules* **1976**, *9*, 206.
(10) Treloar, L. R. G. *The Physics of Rubber Elasticity*, 3rd ed.; Clarendon: Oxford, 1975.
(11) James, H.; Guth, E. *J. Chem. Phys.* **1947**, *15*, 669.
(12) Flory, P. J. *Proc. R. Soc. London, A* **1976**, *351*, 351.
(13) Flory, P. J.; Rehner, J. Jr. *J. Chem. Phys.* **1953**, *11*, 521.
(14) Bastide, J.; Picot, C.; Candau, S. *J. Macromol. Sci., Phys.* **1981**, *B-19*, 13.
(15) (a) Flory, P. J. *J. Chem. Phys.* **1977**, *66*, 5720; *Macromolecules* **1979**, *12*, 119. (b) Erman, B.; Flory, P. J. *J. Chem. Phys.* **1978**, *68*, 5363; *Macromolecules* **1982**, *15*, 800.
(16) Dossin, L. M.; Graessley, W. W. *Macromolecules* **1979**, *12*, 673.
(17) Langley, N. R.; Ferry, J. D. *Macromolecules* **1968**, *1*, 353.
(18) Gottlieb, M.; Gaylord, R. J. *Polymer* **1983**, *24*, 1644; *Macromolecules* **1984**, *17*, 2024.
(19) Marucci, G. *Macromolecules* **1981**, *14*, 434.
(20) Gaylord, R. J. *Polym. Bull. (Berlin)* **1982**, *8*, 325.
(21) Graessley, W. W. *Polym. Prepr. (Am. Chem. Soc., Div. Polym. Chem.)* **1981**, *22*(2), 152.
(22) Ball, R. C.; Doi, M.; Edwards, S. F.; Warner, M. *Polymer* **1981**, *22*, 1010.
(23) Graessley, W. W. *Adv. Polym. Sci.* **1977**, *46*, 140.
(24) Edwards, S. F. *Br. Polym. J.* **1977**, *9*, 140.
(25) Ferry, J. D. *Viscoelastic Properties of Polymers*, 3rd ed.; Wiley: New York, 1980.
(26) Strazielle, C. *Makromol. Chem.* **1958**, *119*, 50.

Kinetics of Phase Separation in Polydisperse Polymer Mixtures

T. E. Schichtel and K. Binder*

Institut für Physik, Johannes Gutenberg Universität Mainz, D-6500 Mainz, Federal Republic of Germany. *Received November 7, 1986*

ABSTRACT: The linearized theory of spinodal decomposition of binary (AB) mixtures is extended to a polymer mixture where both the A chains and the B chains may be polydisperse. The treatment is based on a dynamic generalization of the Flory–Huggins lattice model including vacancies (that model "free volume"), considering the limit where the vacancy concentration is small and the system is brought to a state close to the spinodal curve. It is shown that in this case the amplification factor $R(q)$ of the fluctuations with wavevector q has the same behavior as in the monodisperse mixture; only the prefactors get renormalized by certain combinations of moments over the molecular weight distribution. Experimental consequences of these results are briefly discussed as well as the related case of unmixing of a monodisperse three-component system (polymer A, polymer B_1, and polymer B_2).

1. Introduction

The kinetics of phase separation of fluid binary polymer mixtures triggered by the spontaneous growth of concentration fluctuations ("spinodal decomposition"[1-6]) has found much recent attention, both experimentally[7-20] and theoretically.[21-29] There are two reasons that the study of spinodal decomposition in polymer mixtures is particularly rewarding:

(i) For large molecular weights, unmixing proceeds so slowly that the initial stages where the concentration inhomogeneities are still small are rather conveniently observed,[14-16] and a meaningful comparison with the "linearized" theory describing these initial stages then should be possible,[21-24,26,29] unlike fluid mixtures of small molecules,[6] where one practically always probes the coarsening behavior occurring at the later stages of unmixing.[3,4]

(ii) Due to the mean-field character[23,24,30,31] of the unmixing transition in polymer mixtures, there is a well-defined initial time regime in polymer mixtures where the linear theory should actually be quantitatively valid,[23,24] unlike fluid mixtures of small molecules or solid alloys where nonlinear behavior of the concentration fluctuations is predicted[5] and found[3,4] already during the earliest stages.

Thus, a quantitative comparison between theory[21-29] and experiment[7-20] would be very desirable: first, a significant experimental check of the theory would show whether our current theoretical understanding of the problem is fairly complete; second, fitting the theory to the experimental data then would yield several interesting microscopic parameters characterizing the mixture.

Unfortunately, such an approach is still hampered by the fact that the theory[21-29] always has considered the idealized case of monodisperse polymers only, while in practice polydispersity of the chains[32] must always be accounted for. The polydispersity changes the parameters describing the static scattering in the one-phase region[33] and the spinodal curve and may have a drastic effect on the equilibrium phase diagram, as given by the "coexistence curve" (binodal) of the mixture.[34-36] The present paper now describes an attempt to fill this gap and study the effect of polydispersity on the kinetic factors entering the theory of spinodal decomposition.

For monodisperse binary mixtures of A chains (consisting of N_A "Kuhn segments" of size σ_A) and B chains (consisting of N_B segments of size σ_B), it was predicted that in the initial stages the relaxation of concentration fluctuations at wavevector q is described by the "amplification factor" $R(q)$ described by

$$R(q) = -q^2\Lambda(q)\frac{1}{S_T^{coll}(q)} \tag{1}$$

where $S_T^{coll}(q)$ is a scattering function describing the collective concentration fluctuations of the mixture and $\Lambda(q)$ is an effective Onsager coefficient describing the interdiffusion of the chains. Denoting the volume fraction of the A segments as ϕ and that of the B segments as $1-\phi$ (neglecting "free volume", the mixture is treated as incompressible), one finds for long wavelengths (q^{-1} exceeding the radii of both A coils and B coils)[21-23,37,38]

$$\frac{1}{S_T^{coll}(q)} = \frac{1}{\phi N_A} + \frac{1}{(1-\phi)N_B} - 2\chi + \frac{1}{18}\left(\frac{{\sigma_A}^2}{\phi} + \frac{{\sigma_B}^2}{1-\phi}\right)q^2 \tag{2}$$

Here χ is the Flory–Huggins parameter,[35,38,39] and 2χ is defined as the second derivative of the enthalpy with respect to ϕ, normalized per volume of a Flory–Huggins

0024-9297/87/2220-1671$01.50/0